Evaluation of stress risers severity in spur gears meshing

Spiridon S Crețu

Mechanical Engineering, Mechatronics and Robotics Department, "*Gheorghe Asachi*" Technical University of Iasi, 43 Dimitrie Mangeron Street, Iasi, Romania. E-mail: spiridon.cretu@tuiasi.ro

Abstract. The standards for gears design use the maximum value of the normal stress σ_{zz} , depicted σ_{H}, as critical stress for RCF of gears. This value σ_{H} can't sustain evidences regarding the stress risers influences. The paper uses the von Mises stress σ_{vM} as critical stress responsible for the initiation of RCF. For concentrated contacts analyses the drawback of FEM is the very long computing time and therefore the author used a semi-analytical method (SAM) based on the numerical formulation for the involved equations of linear half-space theory. The finite width of gears' teeth imposes quarter-space limitations and consequently the virtual pressures and correction coefficient were considered in the iterative process for pressures distribution. The pressure distribution was further used to evaluate the stress tensor components and 3D distributions of von Mises stresses. Examples are presented for spur gears with different values for end chamfers.

1.Introduction

Well designed gears, manufactured in good industrial practice and running in conditions to assure an adequate lubrication, are able to avoid common failures as fatigue and static fracture by root bending or various forms of wear, including scuffing, but eventually the rolling contact fatigue (RCF) determines gear's teeth failure [1, 2]. The different pressures risers accelerate the RCF that means shorter lives.

The maximum value σ_{H} of pressures distribution σ_{zz} attained under the pure normal loading figure 1, is used by standards for gears design [3]. This value known as Hertz pressure can't sustain evidences regarding the stress risers influences. Alternative fatigue criteria consider the maximum shear stress τ_{45}, or maximum von Mises stress σ_{vM} as critical stress responsible for the initiation of RCF [4-8]. The equation (1) of von Mises equivalent stress reflects the contribution of each tensor 's component :

$$\sigma_{\mathrm{vM}}(x,y,z)=\frac{1}{\sqrt{2}}\left[\left(\sigma_{xx}-\sigma_{yy}\right)^2+\left(\sigma_{yy}-\sigma_{zz}\right)^2+(\sigma_{zz}-\sigma_{xx})^2+6\left(\tau_{xy}^2+\tau_{yz}^2+\tau_{zx}^2\right)\right]^{1/2} \quad (1)$$

The paper uses the maximum von Mises stress σ_{vM} as critical stress responsible for the initiation of RCF, [9 - 13]. The drawback of FEM applied to concentrated contacts analyses is the very long computing time and therefore the author developed a fast and robust semi-analytical method (SAM).

2. Semi-analytical method

The developed SAM is based on Love's analytical formulation for Boussinesq equation of linear half-space theory and Hartnett approach [9] for numerical formulation:

a) geometric equation of the elastic contact:

$$g_{ij}=h_{ij}+w_{ij}-\delta_0 \quad (2)$$

where: g_{ij} is the gap between the normal loaded surfaces, h_{ij} is the separation between unloaded surfaces, w_{ij} is the elastic deformation of the two surfaces, measured along the normal load, and δ_0 is the rigid displacement of the contacting bodies;

b) equation of the normal surface displacement:

$$w_{ij} = \sum_{k=0}^{Nx-1} \sum_{j=0}^{Ny-1} (K_{i-k,j-l} * p_{kl}) \quad (3)$$

where: the influence coefficients function K_{ij} represents the value of the surface deformation created in the point *(i, j)* by the unit pressure acting in the elementary rectangle *(k, l)*, and $p_{k,l}$ is the unknown value of pressure acting in the same elementary rectangle,

c) load balance equation:

$$\Delta x \Delta y \sum_{i=0}^{Nx-1} \sum_{j=0}^{Ny-1} p_{ij} = F \quad (4)$$

d) conditions regarding non-penetration, non-adhesion and elastic-perfect plastic behaviour are also included.

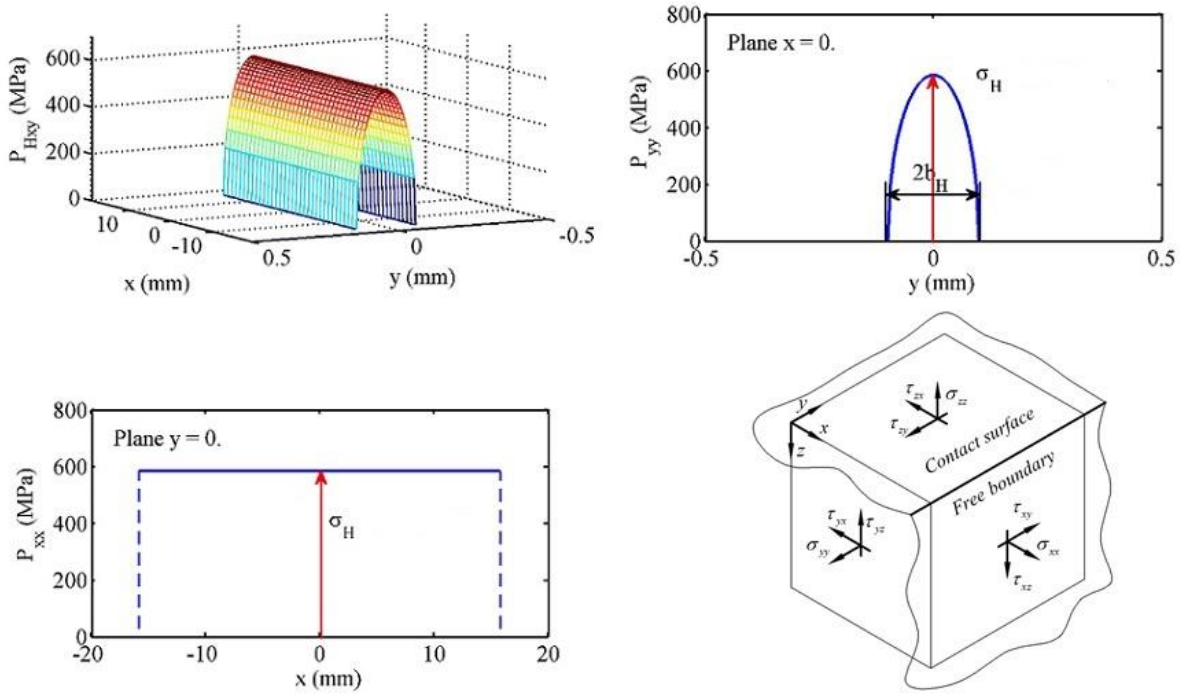

Figure 1. The pressures distributions in the linear half-space based on Hertz's hypothesis.

3. Solution and validation of SAM.

The system of algebraic equations was solved using conjugate gradients methods (GCM) including fast Fourier transform (FFT) to solve the convolution products, [10 - 13].

3.1 Point contacts.

The results obtained with SAM proved to be identical with those calculated using Hertz's formulae, when applicable or provided by FEM if the concentrated contact was a non-Hertz one, figure 2.

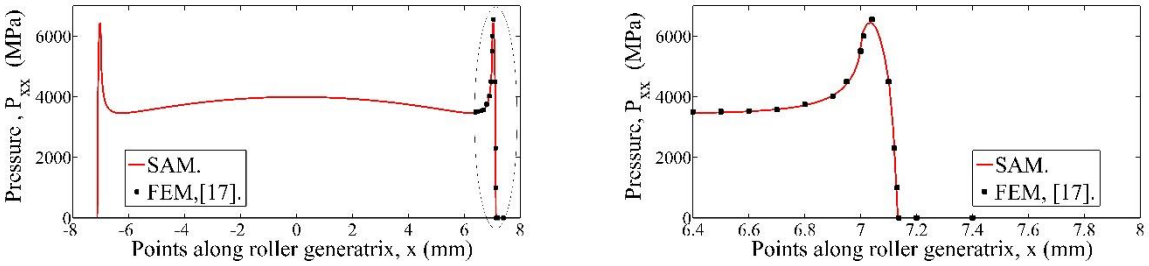

Figure 2. The pressure distributions developed in the normal contact between a crowned cylindrical roller with an end chamfer and a cylindrical inner ring [17].

3.2 Linear contacts and the effect of the finite length.

A real gear with two stress-free sides, has to be modelled as a quarter-space instead of a half-space, figure 1. To eliminate the two shear stresses and one normal stress in the width faces, it was proposed by Hettenyi [18] a two steps correction:

- firstly the application of mirror pressures, figure 3, able to eliminate the two shear stress, and,
- secondly an iterative overlapping half-space solutions till accomplish the boundary condition.

of the quarter-space. Theoretically, the number of iterations goes to infinite but practically the finite number of iterations depends on the accuracy needed. To speed up the entire computation process the virtual pressures and correction coefficient, figure 3 as recently were proposed by Guilbault and Najjari [18], have been considered in the iterative algorithm.

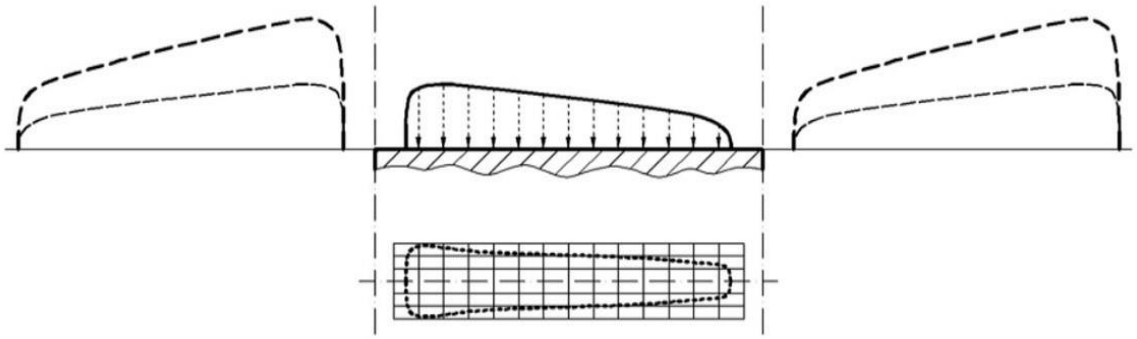

Figure 3. The virtual rectangular contact area and the mesh with coordinate system, [14].

4. The separation matrix

Spur involute gears are in line contact at every instant and a virtual rectangular contact area is built having the contact line as median line. figure 4. Using the involute proprieties the matrix of separations h_{ij} is possible to be expressed analytically for each mesh point (i, j) of the virtual rectangle [14 - 16].

5. Load repartition

The numerical analyses have been performed for a standard spur gars with the following data:

$\alpha_0 = 20^0$, $h_{ao}^* = 1$, $c_0^* = 0.25$, $\rho_0^* = 0.38$

$z_1 = 23$, $z_2 = 51$, $m_n = 4$ mm, $x_1 = 0$, $x_2 = 0$, $B = 32$ mm, $Rch = 0.3$ mm.

The nominal power parameters were: $T_2 = 15$ kW, $\varpi_2 = 53.77$ rad/s.

In this study the non-uniform model of load distribution proposed by Pedrero José et al. [19, 20] has been used. Results obtained with Hertz equations indicated the inner point B of single pair tooth contact as the point where the Hertz pressure σ_H attains the highest value.

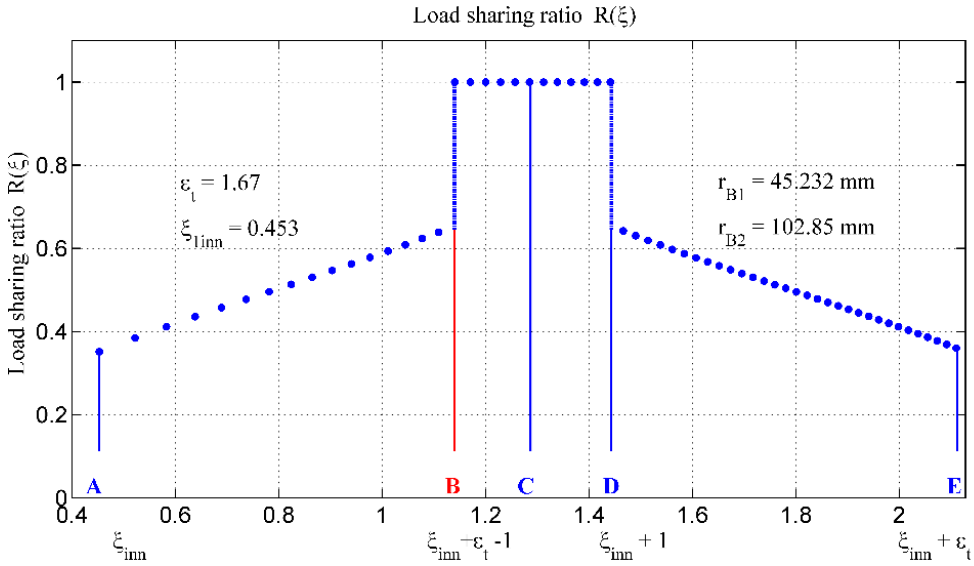

Figure 4. Load sharing ratio, [14].

6. Pressures distribution

The pressures distributions obtained for cases of half space and quarter space hypotheses are presented in figure 5 and figure 6, respectively.

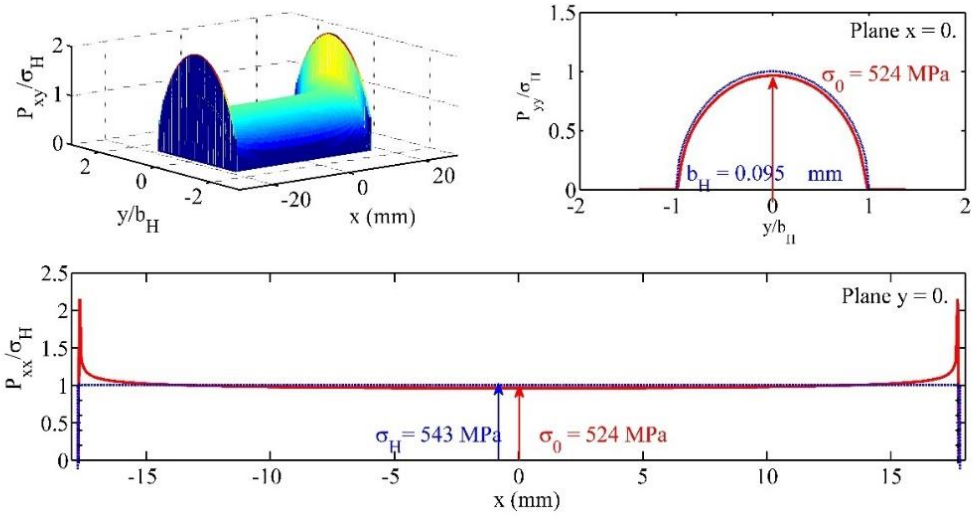

Figure 5. The pressures distribution provided by SAM method within half-space hypothesis.

7. Von Mises equivalent stress distribution

The pressures concentrations accelerate the rolling contact fatigue (RCF) and wear phenomena resulting shorter lives for gears. Popinceanu et al. [4] accomplished a comparative analysis of different components of stress tensor that have been hypothesized as the critical stress in RCF and concluded that von Mises equivalent stress, assures the best correlation with various theoretical and experimental findings. Zhu D. et. al [7], used von Mises stress to predict the pitting life in mixed lubricated line contacts. To evaluate the fatigue life of rolling contacts Morales-Espejel et. al [8] used von Mises equivalent stress in a general model for the surface-subsurface competing RCF mechanism.

8. Stress risers severity

For each infinitesimal volumetric element of significantly stressed volume the new approach takes into account the probability of survival *S* after a number *N* of contact cycles,[5, 6]:

$$\ln\frac{1}{S}\sim N^{e}\iiint_{0}^{V}\frac{\left(\sigma_{eq}-\sigma_{u}\right)^{c}}{z'^{h}}dV \tag{5}$$

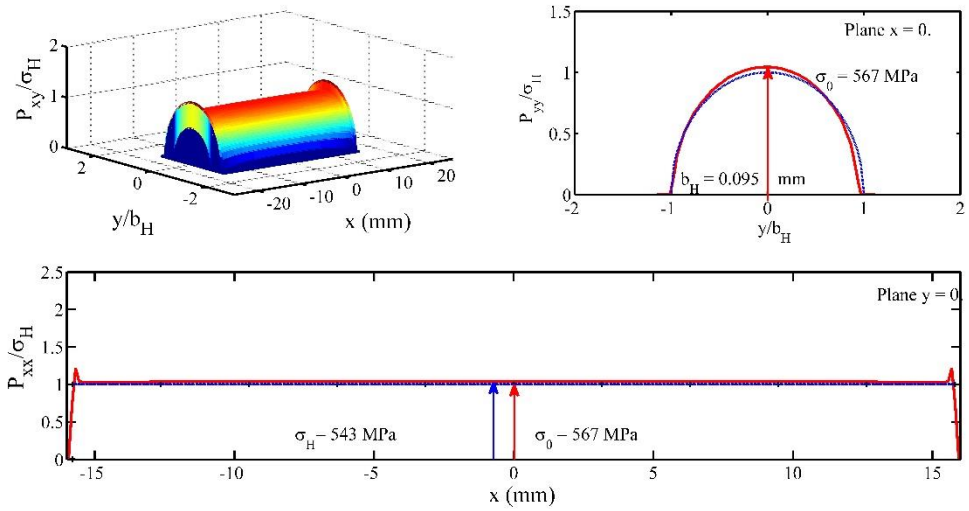

Figure 6. The pressures distribution provided by SAM method within quarter-space hypothesis.

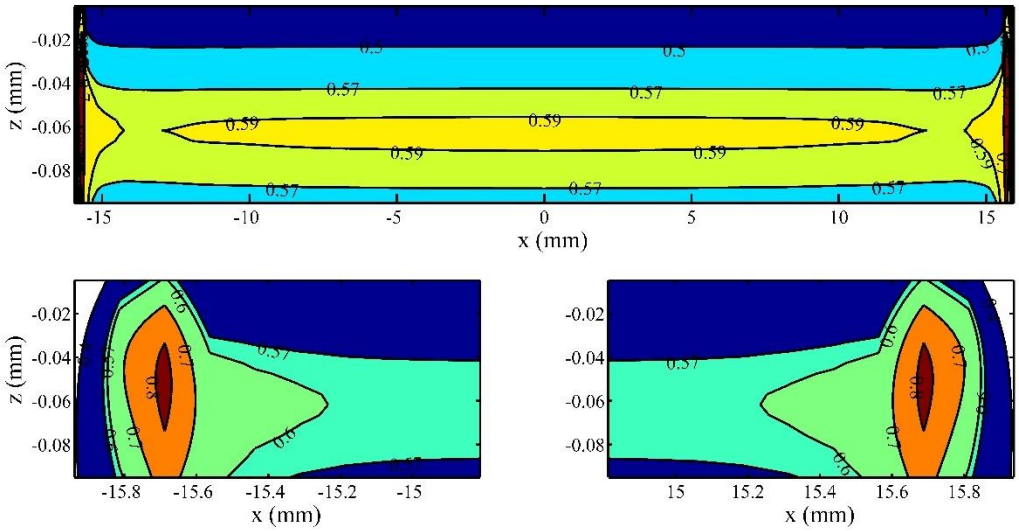

Figure 7. The depth distribution of von Mises stresses created by pressures depicted in figure 6.

where $\boldsymbol{\sigma_{eq}}$ is the equivalent stress value in the infinitesimal volumetric element, $\boldsymbol{\sigma_u}$ is the fatigue limit stress, $\boldsymbol{c}$ is the stress exponent, $\boldsymbol{z'}$ is the stress-weighted average depth, $\boldsymbol{h}$ is the depth exponent, $\boldsymbol{e}$ is the Weibull slope and $\boldsymbol{V}$ is the volume significantly stressed. For an imposed value of reliability the integration of last equation over the significant stressed volume lead to a correspondent number of loading cyles until rolling contact fatigue is evidenciated. The same operations done to the similar

loading and geometrical conditions, but with no stress riser, provides the maximum number of loding cycles for the particular gear. The ratio of the two durabilities will represent the severity number.

9. Conclusions

The large industrial experience as well as a lot of experimental works pointed out the lack of Hertz stress to provide consistent explanations for important experimental outcomes. Theoretical and experimental studies proved that von Mises equivalent stress offers good explanations for the experimental and theoretical findings and provides a solid formulation to calculate the gears life as long as a value for reliability is chosen. The stress riser severity is proposed as the ratio between the optimum life obtained with no stress riser and the life obtained when the stress riser exists.

References

[1] Santus C, Beghini M. Bartilotta I and Facchini M, 2012, *Int. J. Fatigue,* **45**, 71-81.
[2] Nelias D, Dumont M.L, Champiot F, Vincent A, Girodin D, Fougeres R, and Flamand L,1999, *ASME Trans. J. Tribol.* ***128***, 240-251,1999.
[3] ISO 6336-1-5, 2006, *Calculation of load capacity of spur and helical gears*, Geneva, Switzerland.
[4] Popinceanu N, Diaconescu E and Crețu S, 1981, *WEAR*, **71**,265-82.
[5] Ioannides E and Harris A T, 1985, *ASME Trans.J.. Tribol.*,**107,**367-78.
[6] Ioannides E, Bergling G and Gabell A, 1999, *Acta Polytech. Scand.*, Mech. Eng. Series, **137,** Finnish Institute of Technology.
[7] Zhu D, Ren N and Wang Q J, 2009, *ASME Trans. J. Tribol.***131**, 4, 1-8.
[8] Morales-Espejel G E, Gabelli A and DeVries A J, 2015, *Tribol. Trans.*, **58**, 5, 894-96.
[9] Hartnett J M, 1979, *ASME Trans. J. Lub. Tech.*, 1979, **101,** 1, 106-109.
[10] Polonsky I A and Keer L, 2000, *ASME Trans.J. Tribo,l.* **122,** 1.
[11] Creţu S, Antalucă E and Creţu O, 2003, *Annals Univ. Galaţi* Romania **24**, 26-35.
[12] Creţu S, 2005, *Bull. Inst. Polit. Iași*, **LI, (LV)**, 1-2, 1-31.
[13] Creţu S, 2009, *Contactul concentrat elastic-plastic*, Ed. Politehnium, Iași, Romania,
[14] Crețu S, Pop N, Cazan S, 2017, MATEC Web of Conferences **112,** 07015, Ian E&E, May 25-26, Iași, Romania.
[15] Litvin Fand Fuentes A, 2004, *Gear geometry and applied theory*, Cambridge Univ. Press, 2
[16] Pop N, Tufescu A and Cretu S, 2014, *App. Mech. Mat.* **658**, 531-56.
[17] de Mul J M, Kalker J J and Fredriksson B, 1986, *ASME Trans. J. Lub. Tribol*., **108**,140-48.
[18] Guibault R, 2011, *ASME Trans. J. Tribol.* **133**, 2.
[19] Pedrero I J, Pleguezuelos M and Artes M, 2010, Mech. Mach..Theory, **45**, 780-74.
[20] Pedrero I J, Pleguezuelos M, Munoz M, 2011, Mech. Mach. Theory, **46**, 425-47.